6-2007

LP 133-373: A New Chromospherically Active Eclipsing dMe Binary with a Distant, Cool White Dwarf Companion

T. R. Vaccaro
Florida Institute of Technology

M. Rudkin
Florida Institute of Technology

A. Kawka
Czech Academy of Sciences

S. Vennes
Florida Institute of Technology

Terry D. Oswalt
Florida Institute of Techology, oswaltt1@erau.edu

See next page for additional authors

The Astrophysical Journal, 661:1112–1118, 2007 June 1

LP 133-373: A NEW CHROMOSPHERICALLY ACTIVE ECLIPSING dMe BINARY WITH A DISTANT, COOL WHITE DWARF COMPANION

T. R. Vaccaro,[1] M. Rudkin,[1] A. Kawka,[2] S. Vennes,[1] T. D. Oswalt,[1] I. Silver,[1] M. Wood,[1] and J. Allyn Smith[3]

Received 2006 December 2; accepted 2007 March 1

ABSTRACT

We report the discovery of the partially eclipsing binary LP 133-373. Nearly identical eclipses along with observed photometric colors and spectroscopy indicate that it is a pair of chromospherically active dM4 stars in a circular 1.6 day orbit. Light and velocity curve modeling to our differential photometry and velocity data show that each star has a mass and radius of $0.340 \pm 0.014\ M_{\odot}$ and $0.33 \pm 0.02\ R_{\odot}$. The binary is itself part of a common proper motion pair with LP 133-374, a cool DC or possible DA white dwarf with a mass of 0.49–0.82 $M_{\odot}$, which would make the system at least 3 Gyr old.

Subject headings: binaries: eclipsing — stars: activity — stars: individual (LP 133-373, LP 133-374) — stars: late-type — white dwarfs

Online material: color figures, machine-readable tables

1. INTRODUCTION

The star LP 133-373 (NLTT 36188)—R.A. (J2000.0) = $14^{h}4^{m}9.0^{s}$, decl. (J2000.0) = $+50^{\circ}20'38''$—was originally listed in the Luyten (1979) catalog as a red star ($R = 15.2$ mag) with a fainter ($R = 17.7$ mag) white dwarf star (LP 133-374, NLTT 36191) as a common proper motion companion separated by 5″. Figure 1 shows a finder chart for these stars.

LP 133-373 was found to be a partially eclipsing binary during unfiltered CCD-based time series photometry of the field in an attempt to detect variability of the white dwarf (Rudkin 2003; Oswalt et al. 2005). Their original estimate of the binary period (0.81 days) corresponds to half of the correct period (1.63 days) because the similarity of the stellar types yields nearly identical light curves for primary and secondary eclipses. This conclusion is supported by detailed light curve modeling and the splitting of emission, as well as absorption lines near quadrature. Light curve variations outside of eclipse indicate dark surface spots that are consistent with the chromospheric activity observed in the spectra (Balmer and Ca II emissions).

Only a few eclipsing low-mass binaries in detached systems have been studied in detail. Lopez-Morales & Shaw (2006) and Shaw & Lopez-Morales (2006) report nine such systems. Other recent identifications were made by Bayless & Orosz (2006), Hebb et al. (2006), and Young et al. (2006). Late-type M dwarf stars are prominent members of the class of eclipsing cataclysmic variables. However, the late-type star is often outshined by the white dwarf's accretion disk, providing little or no mass, luminosity, or radius information, crucial in understanding the physical and evolutionary nature of these stars. Reviews of late-type mass-radius relations are given by Caillault & Patterson (1990), Chabrier & Baraffe (2000), and Reid & Hawley (2000).

We present in § 2 new observations of the common proper motion pair LP 133-373/LP 133-374, and in particular photometric and spectroscopic data confirming that LP 133-373 is itself an eclipsing late-type binary. Detailed orbital and stellar properties of the binary LP 133-373 are derived in § 3.1 and an analysis of the common proper motion companion LP 133-374 is presented in § 3.2. We summarize and conclude in § 4.

2. OBSERVATIONS

2.1. *Photometry*

We recently reprocessed the original photometric measurements obtained by Smith (1997) on 1994 April 2 at the Kitt Peak National Observatory (KPNO) 0.9 m telescope. See Smith (1997) for more details. We remeasured the *BVRI* colors for the red dwarf and white dwarf components, respectively: $B = 16.907 \pm 0.029$ mag, $V = 15.319 \pm 0.014$ mag, $R = 14.093 \pm 0.012$ mag, $I = 12.476 \pm 0.013$ mag, and $B = 18.587 \pm 0.029$ mag, $V = 18.020 \pm 0.053$ mag, $R = 17.387 \pm 0.027$ mag, $I = 16.274 \pm 0.029$ mag. The white dwarf colors were differentially determined with a field star, and the red star's photometry was obtained with an aperture that excluded the white dwarf. The red dwarf data were obtained out of eclipse. The colors clearly show that the red star is approximately of dM4–5 spectral type, in agreement with the spectra, which exhibit chromospheric activity and provide measurements of the TiO5 bandheads, indicating a dM4 classification (see Fig. 2) in agreement with previous classifications (Silvestri et al. 2005). Our comparisons of the available colors with other dM stars in the literature (Cox 2000; Reid & Hawley 2000) also place it in the dM4 range, which we assume for our analysis.

Series of images of LP 133-373 were taken with the 0.9 m telescope of the Southeastern Association for Research in Astronomy (SARA), which is also located at KPNO. The initial eclipsing data were obtained in 2003 May, using SARA's Ap7P CCD and no filters. Differential light curves were produced from the 2003 through 2005 observing seasons using various comparison stars in the field. Since the data were collected and reduced by several different observers using different comparison stars during this time, and due to the unfiltered nature of the photometry, these light curves served only to establish the ephemeris. Observations made on the (UT) nights of 2006 May 2, 3, 4, 21, and 30 were taken with SARA, using the Finger Lakes CCD with Johnson *R* and *I* filters. A consistent comparison was used,

[1] Department of Physics and Space Sciences and SARA Observatory, 150 West University Boulevard, Florida Institute of Technology, Melbourne, FL 32901; tvaccaro@fit.edu, mrudkin@fit.edu, svennes@fit.edu, toswalt@fit.edu, isilver@fit.edu, wood@fit.edu.

[2] Astronomický ústav AV ČR, Fričova 298, CZ-251 65 Ondřejov, Czech Republic; kawka@sunstel.asu.cas.cz.

[3] Department of Physics and Astronomy, Austin Peay State University, Clarksville, TN 37044; smithj@apsu.edu.

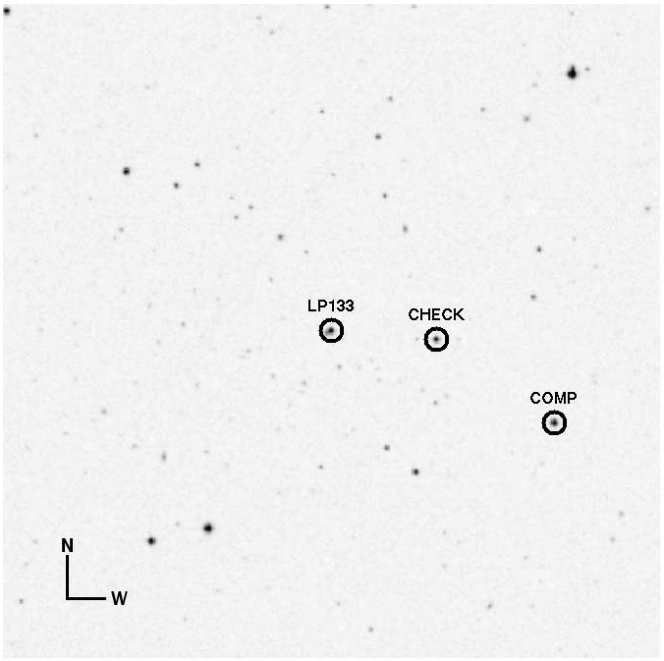

FIG. 1.—Finder chart (red POSSII) for LP 133-373/LP 133-374 from the STScI Digitized Sky Survey indicating the binary LP 133-373, the comparison, and check stars with circles. The distant white dwarf (LP 133-374) is barely visible to the southeast of the brighter binary. The image is $10' \times 10'$.

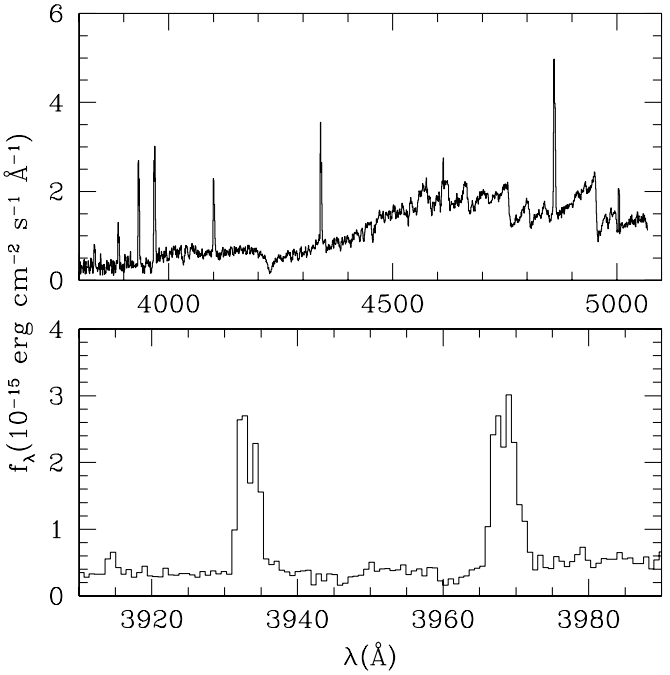

FIG. 2.—*Top*: Mayall 4 m KPNO spectrum of LP 133-373 (HJD = 2,453,580.703). *Bottom*: Ca II H and K emission lines can be seen split as the binary was near quadrature.

along with a check star that was always in the field to get differential measurements. Typical exposures were 30 s, which yielded a S/N $\approx$ 40. These stars are shown in Figure 1.

All new photometric data were reduced using standard procedures within IRAF[4] and measured with apertures a few arcseconds wide so as to exclude the white dwarf, which may have contributed less than 1% in *R* or *I* in some cases. However, we believe that observations in these pass bands for the white dwarf reported by Smith (1997) are contaminated by LP 133-373; therefore, we rely on the Sloan Digital Sky Survey (SDSS) *ugriz* photometry for the white dwarf, which yields $u = 20.018 \pm 0.038$ mag, $g = 18.797 \pm 0.008$ mag, $r = 18.256 \pm 0.007$ mag, $i = 18.004 \pm 0.009$ mag, and $z = 18.076 \pm 0.020$ mag. Sloan data for the red dwarf were marked as saturated and could not be used.

Finally, we obtained Two Micron All Sky Survey (Skrutskie et al. 2006; 2MASS) *JHK* photometry of the binary LP 133-373: $J = 10.905 \pm 0.020$, $H = 10.306 \pm 0.021$, and 10.091 ± 0.015. The data are useful as an independent verification of the average M dwarf absolute luminosity. The start and end of the observations are HJD 2,451,322.699946 and HJD 2,451,322.704645, respectively, and according to our ephemeris (see § 3.1 and Table 1) the data were obtained out of eclipse (phase = 0.7).

2.2. *Spectroscopy*

2.2.1. *KPNO 1989 February*

Spectra of the white dwarf LP 133-374 and red dwarf LP 133-373 were originally obtained with the Ritchey-Chrétien (RC) spectrograph attached to the 4 m telescope at KPNO on 1989 February 7 (UT). We obtained a single exposure of 1200 s with both stars on the slit. The BL250 grating (158 lines mm^{-1}) and TI-2 CCD (15 μm pixel size, circa 1989) were used to obtain a spectral range of 3500–6200 Å with a dispersion of 3.45 Å pixel^{-1} and a resolution of $\approx$14 Å. The resulting signal-to-noise ratio reached 15 in the red dwarf spectrum near 4150 Å, and 5 throughout the white dwarf spectrum. The white dwarf spectrum appears featureless to the noise limit. The spectrum is also relatively red, indicating a low effective temperature at which hydrogen Balmer lines are expected to be weak. The white dwarf is tentatively classified as a DC. A DA classification remains possible and would be confirmed with the acquisition of a high signal-to-noise ratio Hα spectrum. The red dwarf spectrum revealed emission lines characteristic of chromospherically active stars.

2.2.2. *KPNO 2005 July*

We obtained two optical spectra of LP 133-373 with exposure times of 1800 s on 2005 July 29 UT at the Mayall 4 m telescope at KPNO. We used the RC spectrograph using the BL450 grating in the second order, resulting in a dispersion of 0.70 Å pixel^{-1} and a resolution of 1.8 Å. The 2k $\times$ 2k T2KB CCD camera with 24 μm pixel size imaged the spectra. An 8 mm $CuSO_4$ order-blocking filter was used to decrease the likelihood of order overlap

TABLE 1
LP 133-373 PARAMETERS ($q \equiv 1.0$)

Parameter	Value
T_0	HJD 2452760.70502 $\pm$ 0.00013
P (days)	1.6279866 $\pm$ 0.0000004
a ($R_\odot$)	5.10 $\pm$ 0.22
i (deg)	85.3 $\pm$ 0.05
T_1 (K)	3058 $\pm$ 195
T_2 (K)	3144 $\pm$ 206
$M_{\rm bol,\,1}$	10.0 $\pm$ 0.5
$M_{\rm bol,\,2}$	9.8 $\pm$ 0.5
Ω_1	16.51 $\pm$ 0.12
Ω_2	16.34 $\pm$ 0.094
R_1, R_2 ($R_\odot$)	0.330 $\pm$ 0.014
M_1, M_2 ($M_\odot$)	0.34 $\pm$ 0.02

[4] IRAF is distributed by the National Optical Astronomy Observatories, which are operated by the Association of Universities for Research in Astronomy, Inc., under cooperative agreement with the National Science Foundation.

within the blue end of the spectrum. The range of wavelengths covered was 3800–5100 Å. We caught the stars near quadrature (HJD = 2,453,580.67333196 or phase = 0.67, and HJD = 2,453,580.70308391 or phase = 0.69), as predicted by the ephemeris generated from the early photometric data. Figure 2 shows prominent emission lines of H I and Ca II H and K. The Ca II H and K and the Balmer lines were split, indicating a velocity separation between the two binary components of ≈144 km s^{-1}. Further details are presented in the analysis section (§ 3.1).

2.2.3. *APO 2006 September*

LP 133-373 was observed using the Dual Imaging Spectrograph (DIS) attached to the 3.5 m telescope at the Apache Point Observatory (APO) on 2006 September 30 02:31:24.7 UT and 02:47:16.0 UT (midexposure times). The exposure time of each spectrum is 900 s. We used the 830.8 line mm^{-1} grating to obtain a spectral range of 6440–8150 Å with a dispersion of 0.84 Å pixel^{-1} in the red. We also used the 1200 line mm^{-1} grating to obtain a spectral range of 3830–5030 Å with a dispersion of 0.62 Å pixel^{-1} to obtain a spectrum in the blue. The slit was set for 1.5″, resulting in a resolution of 2.1 Å in the red and 1.7 Å in the blue. For each spectrum, the signal-to-noise ratio reached 5 near 4150 Å and 20 near Hα.

Previous spectra had been obtained at APO (Silvestri 2002; Silvestri et al. 2005) on 2001 February 4 09:59:13 UT (midexposure) but did not show double lines because the orbit was near conjunction (phase = 0.9). Our more recent APO spectra (2006 September 30), taken nearly an hour after eclipse (phase = 0.53), yields an Hα emission velocity $v(\mathrm{H}\alpha) = -32.0 \pm 5.0$ km s^{-1}, which should closely match the systemic velocity, but the expected line split (≈20 km s^{-1}) at this time was not detected due to limited resolution (≈100 km s^{-1}). Further details are presented in the analysis section (§ 3.1).

All new spectroscopic data were reduced using standard procedures within IRAF. Heliocentric corrections were applied to the wavelength scale of all spectra.

3. ANALYSIS

3.1. *The Eclipsing Binary LP 133-373*

To determine the binary parameters we followed four steps. First, we used the epoch of all seven eclipses, which include four eclipses observed using unfiltered CCD data taken during 2003–2005 and three eclipses observed using filtered photometry in 2006 May, and we determined the initial epoch of the primary mideclipse and the orbital period (Table 1). Figure 3 shows the *O-C* diagram for the epoch of all seven eclipses. Significant deviations with respect to our ephemeris are evident. We attribute these deviations to the presence of surface spots with varying contrasts and locations. The epoch of primary eclipse is (HJD)

$$T = 2{,}452{,}760.70502 \pm 0.00013 + E\ 1.6279866 \pm 0.0000004 \text{ days}$$

In a second step, we used the ephemeris as a starting point for the binary star program PHOEBE (Prša & Zwitter 2005) and we performed detailed light curve modeling of our *R* and *I* data taken in 2006 May. We do not model unfiltered data. The program PHOEBE is based on the Wilson-Devinney (WD) program (Wilson & Devinney 1971; Wilson 1979, 1990). The similarity in the primary and secondary eclipses led us to adopt a mass ratio of 1.0, a circular orbit, and typical dM4 temperatures (Cox 2000; Reid & Hawley 2000) for each star of 3100 K.

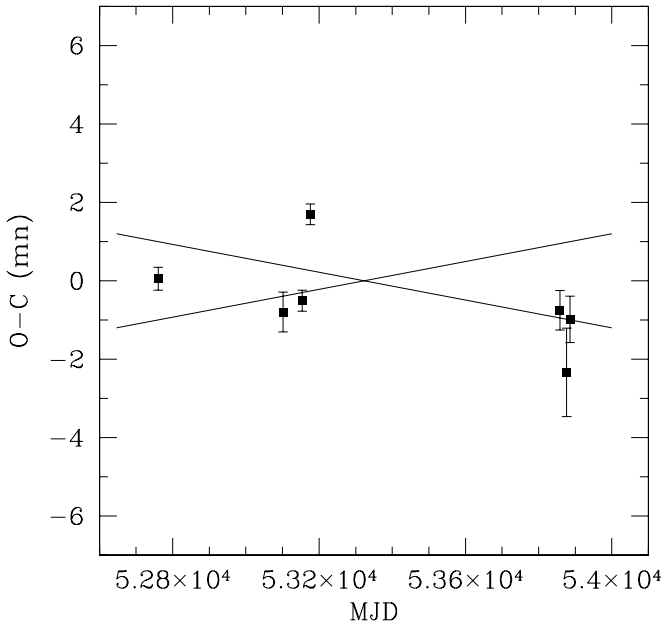

FIG. 3.—The *O-C* diagram showing deviations of the epoch measurements (in units of minutes) of seven usable eclipses relative to the adopted ephemeris vs. the epoch (MJD). The solid lines show expected deviations from the ephemeris if the period is increased or decreased by 5 σ (0.000002 days).

The radial velocity measurements provide the only anchor in establishing the semimajor axis *a*. Radial velocities were determined from our 2005 July spectroscopy, which included measurements from Hβ, Hγ, Hδ, and Ca II K emission lines while excluding the very blended lines of Hϵ and Ca II H. The line centers were measured using IRAF's routine for deblending multiple profiles, in this case two profiles—one for each star. Only two sets of heliocentric velocities were obtained at phase = 0.67, $v_1 = -108.2 \pm 4.4$ km s^{-1} and $v_2 = 31.1 \pm 4.1$ km s^{-1}, and phase = 0.69, $v_1 = -100.9 \pm 6.3$ km s^{-1} and $v_2 = 47.6 \pm 7.2$ km s^{-1}. The average velocity separation is 144 ± 8 km s^{-1}. A best fit to the velocities starting with the known period, a systemic velocity between the measured velocities ≈−33 km s^{-1} (which is close to the APO measurement of $v = -32.0 \pm 5.0$ km s^{-1} at phase 0.53), and an inclination of 90° yields a minimum total mass of the system ≳0.67 $M_\odot$.

We repeated the radial velocity analysis using the absorption line spectra. We adopted the spectrum of the dM3.5 star Gliese 15B as a template for both component stars of LP 133-373. The spectrum of Gliese 15B was obtained at KPNO on 2006 November 27 with the same instrumental setup used on 2005 July. We established the zero-velocity scale using the radial velocity measurement of Nidever et al. (2002), $v(\mathrm{Gl15B}) = 11.0 \pm 0.4$ km s^{-1}. We shifted the two templates independently within a velocity range of −200 to +200 km s^{-1} and fitted the combined templates to the observed spectrum of LP 133-373 using a χ^2-minimization technique. The best fits for the 2005 July spectra resulted in $v_1 = -94 \pm 10$ km s^{-1} and $v_2 = 46 \pm 10$ km s^{-1} (phase = 0.67), and $v_1 = -90 \pm 10$ km s^{-1} and $v_2 = 60 \pm 10$ km s^{-1} (phase = 0.69), which corresponds to an average velocity separation of 145 ± 14 km s^{-1}. The velocity separation measurements using absorption and emission-line spectra are essentially identical. We also measured the systemic velocity in the APO 2006 September spectrum (−24 ± 7 km s^{-1}) using K I resonance lines at $\lambda = 7664.911$ and 7698.974 Å. We find that the mass ratio (M_2/M_1) ranges from ≈1.0 using the emission spectra to ≈1.1 using the absorption spectra. Although we adopted

TABLE 2
LP 133-373 Spot Solutions in 2006 May Data

Spot Number	Co-Latitude (radians)	Longitude (radians)	Angular Radius (radians)	Temperature Factor ($T_{spot}/T_{photosphere}$)
1.....	0.70 ± 0.17	0.00 ± 0.04	0.40 ± 0.02	0.72 ± 0.06
2.....	0.55 ± 0.07	5.30 ± 0.06	0.45 ± 0.03	0.78 ± 0.05

$M_2/M_1 = 1$, we will explore the effect of a varying mass ratio (see below).

Next, in a third step, the inclination and potentials (stellar radii) were then iteratively adjusted within PHOEBE until both eclipse depths and widths matched the observed light curve. Note that all solutions are based on an atmosphere of 3500 K ramped from a blackbody approximation at 1500 K, and on logarithmic limb darkening with coefficients by van Hamme (1993) for temperatures of 3500 K, since the coefficient values are not known below this temperature. Table 1 presents the simultaneous light/velocity solutions.

Finally, in a fourth and final step we introduced surface spots. Initial fits were done with the light levels adjusted to match the eclipses. We subsequently scaled the model light curve to values outside of eclipse (near phase 0.25), and spots were added to fit the complete light curve since a spot wave is clearly evident. Light curve models were compared to the eclipse geometry implied by our *R*, *I*, and unfiltered photometry. The unfiltered comparisons are only for a check on the ephemeris, since spot configurations are surely different between the 2003 and 2006 epochs. We fit our photometric data with model light curves using the spot parameters given in Table 2. No satisfactory fit was possible without starspots, so cool spots were added one at a time, with typical temperature factors, $T_{spot}/T_{photosphere}$, of about 0.80. Spots on the facing hemisphere of each star were needed. A similar effect on the light curves would occur if the spots were on the outer facing hemispheres, but the models were best fit with the inner facing configuration. The spot parameters were refined with the differential-corrections-routine part of the Wilson-Devinney code. Figure 4 shows the light curve using parameters for the two spots given in Table 2, and Figure 5 shows the binary configuration at four phases ($\Phi = 0.0,\ 0.25,\ 0.5,$ and 0.75) and as seen along the line of sight.

We also examined the sensitivity of the solutions to our assumption of a mass ratio $q = 1$. If we let the mass ratio reach $q = 0.9$ and 1.1, in both cases the separation increases from 5.1 to 5.15 $R_\odot$, corresponding to a slight increase in the total systemic mass from 0.68 to 0.69 $M_\odot$ and no significant effect on the inclination. Of course, by introducing a mass asymmetry, the predicted systemic velocity shifts from −33 to −29 km s^{-1} at $q = 0.9$ and to −40 km s^{-1} at $q = 1.1$. The solutions closely match the limits allowed by our systemic velocity measurement of $v = -32.0 \pm 5.0$ km s^{-1}, and therefore the actual mass ratio should be found within the range $q = 0.9$–1.1.

Tables 3 and 4 present our photometry, where ΔR and ΔI refer to magnitude differences between LP 133-373 and the comparison star shown in Figure 1.

3.1.1. *Luminosity and Distance Estimate of the Red Dwarf*

We computed the distance to the binary several ways. This allowed us to check the modeled binary luminosity for consistency and to find the luminosity of the white dwarf common proper motion component. Two methods of determining luminosity for the binary from observable measurements were used. One method uses the $V-I$ colors to obtain the absolute visual magnitude M_V.

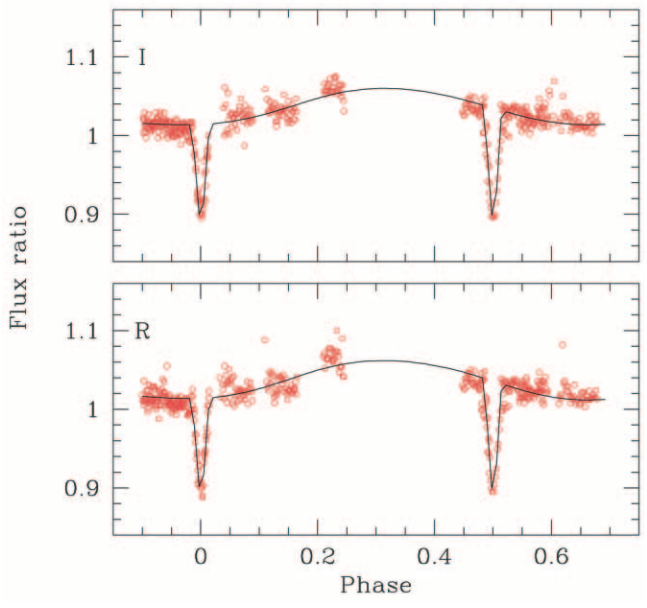

Fig. 4.—Light curve model (*solid lines*) compared with our *I*-band (*top*) and *R*-band (*bottom*) photometry (*open circles*).

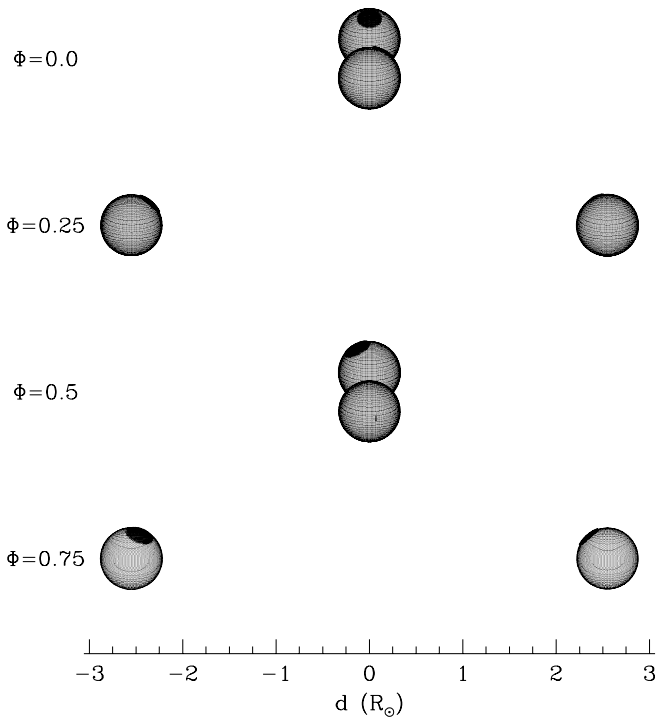

Fig. 5.—Binary configuration as seen along the line of sight at $\Phi = 0.0$, 0.25, and 0.5. The images were generated with PHOEBE.

TABLE 3
PHOTOMETRIC R DATA FOR LP 133-373

HJD (−2,453,800)	ΔR
57.74370	−0.024
57.74743	−0.004
57.74804	−0.012
57.74863	−0.016
57.75122	−0.015
57.75182	−0.018
57.75241	−0.013
57.75499	−0.024
57.75559	0.003
57.75618	−0.018

NOTE.—Table 3 is published in its entirety in the electronic edition of the *Astrophysical Journal*. A portion is shown here for guidance regarding its form and content.

The other method utilizes the TiO5 band strength to get M_V. The apparent magnitude (m_V) can then be used to compute a distance modulus. We assumed that the stars were identical enough to facilitate a simple distance correction. The inverse square law allows us to correct the distance computed for two identical stars by treating them as one and multiplying the result by $\sqrt{2}$.

The empirical color magnitude diagram of nearby stars yields the following relationship for $0.85 < V - I < 2.85$ (Reid & Hawley 2000):

$$M_V = 3.98 + 1.437(V - I) + 1.073(V - I)^2 - 0.192(V - I)^3,$$

with $\sigma(M_V) = 0.5$. Using our $(V - I) = 2.843$, we get an $M_V = 12.3$, which gives a distance of 40 pc for a single star of this color and observed $V = 15.319$. However, we correct this distance by a factor of $\sqrt{2}$ and find the distance to the system to be 56 pc.

A similar relationship exists for the TiO5 band strength (Reid et al. 1995),

$$M_V = 25.33 - 53.15(\mathrm{TiO5}) + 64.1(\mathrm{TiO5})^2 - 29.14(\mathrm{TiO5})^3,$$

TABLE 4
PHOTOMETRIC I DATA FOR LP 133-373

HJD (−2453800)	ΔI
57.74927	−0.010
57.74988	−0.010
57.75048	−0.030
57.75305	−0.030
57.75364	−0.011
57.75424	−0.008
57.75683	−0.013
57.75803	−0.015
57.76063	−0.003
57.76122	−0.024

NOTE.—Table 4 is published in its entirety in the electronic edition of the *Astrophysical Journal*. A portion is shown here for guidance regarding its form and content.

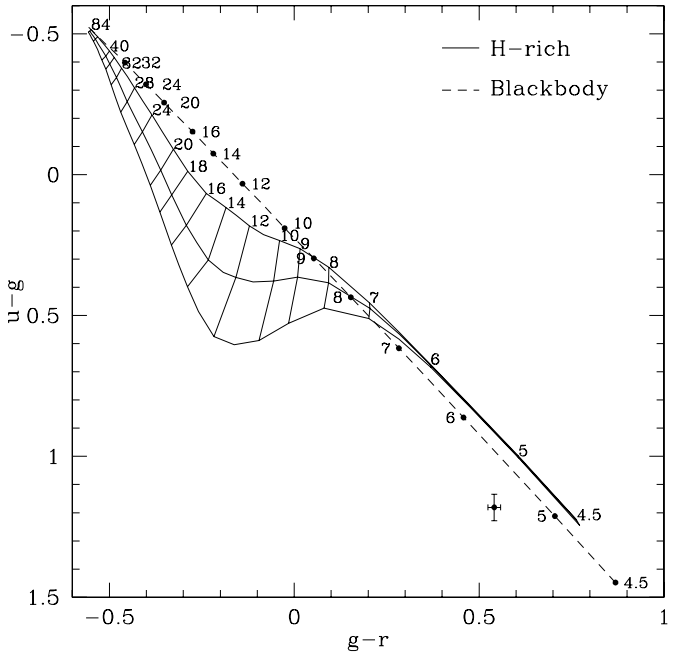

FIG. 6.—SDSS $(u - g)$ vs. $(g - r)$ photometry of LP 133-374 (*filled circle with error bars*) compared to synthetic colors of hydrogen-rich white dwarfs (*solid line*) and blackbody (*dashed line*). The effective temperature is indicated in units of 1000 K and for hydrogen-rich colors log $g = 7.0$, 8.0, and 9.0 (*bottom to top*). The grid shown does not include the effect of missing blue/ultraviolet opacity. [*See the electronic edition of the Journal for a color version of this figure.*]

with $\sigma(M_V) = 0.5$. Using TiO5 = 0.37 (Silvestri 2002) we get $M_V = 13.0$ and a distance of 30 pc, which when corrected for two stars becomes 42 pc.

The PHOEBE light curve models compute bolometric magnitudes for both stars, which are similar ($M_{\mathrm{bol}} \approx 9.9 \pm 0.5$). Bolometric corrections for the visual bandpass can be computed and subtracted from the modeled M_{bol} to give M_V using the following relation (Reid & Hawley 2000):

$$\mathrm{BC}_V = 0.27 - 0.604(V - I) - 0.125(V - I)^2,$$

which gives us $\mathrm{BC}_V = 2.5$, and therefore $M_V = 12.4$ for a corrected distance of 55 pc. The model is consistent with the two independently determined distance estimates ranging from 42 to 56 pc.

In summary, the distance estimates imply a modulus of

$$m - M = 3.4 \pm 0.3.$$

Adopting $m_K - M_K = 3.4 \pm 0.3$, the absolute magnitude $M_K = 6.7 \pm 0.3$ for the pair or $M_K = 7.4 \pm 0.3$ for each binary component assuming equal luminosity. The measured $V - K = 5.23 \pm 0.03$ and our M_K estimate for LP 133-373 are consistent with established relations for nearby stars (Reid & Hawley 2000). The main limitation to the usefulness of such relations is the intrinsic scatter found in color-luminosity measurements. Note that the absolute *JHK* magnitudes of the nearby white dwarf companion (see § 3.2) are ≳13 mag; Therefore, potential contamination of the infrared data by the white dwarf is insignificant.

3.2. *Physical Parameters and Age of the White Dwarf LP 133-374*

To analyze the photometric and spectroscopic data of the white dwarf LP 133-374, we calculated a set of synthetic SDSS *ugriz* colors using a grid of pure-hydrogen models (Kawka &

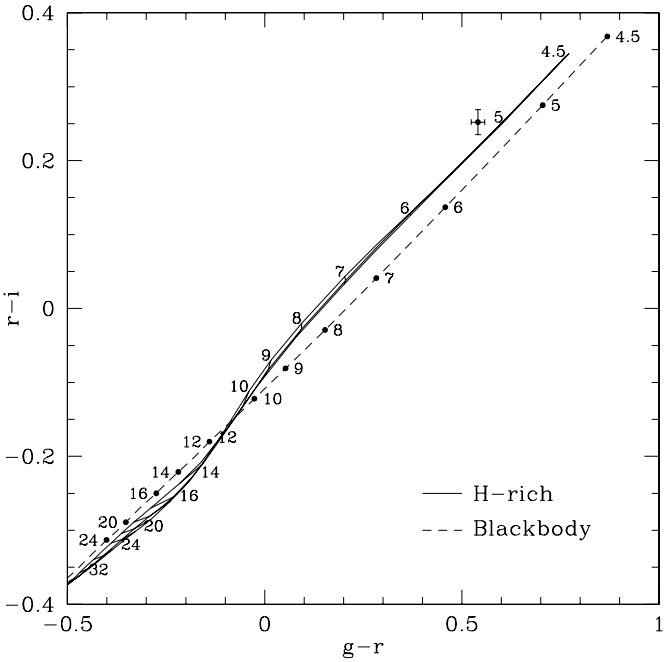

FIG. 7.—SDSS $(r-i)$ vs. $(g-r)$ photometry of LP 133-374 compared (*filled circle with error bars*) to synthetic colors of hydrogen-rich white dwarfs (*solid line*) and blackbody (*dashed line*). The effective temperature is indicated in units of 1000 K and for hydrogen-rich colors $\log g = 7.0$, 8.0, and 9.0 (*bottom to top*). [*See the electronic edition of the Journal for a color version of this figure.*]

Vennes 2006) for $T_{\rm eff} = 4500$–84,000 K and $\log g = 7.0$, 8.0, and 9.0. We also calculated synthetic *ugriz* colors for blackbody spectra with temperatures ranging from $T_{\rm eff} = 4500$ to 84,000 K. Figures 6 and 7 show the observed $(u-g)$ versus $(g-r)$ and $(r-i)$ versus $(g-r)$ colors, respectively, compared to the synthetic colors for pure-hydrogen models and the blackbody colors.

Note that Kowalski & Saumon (2006) recently established that the extended line wing of Lyα contributes significantly to the total opacity in the blue part of the optical spectrum. The additional opacity is due to perturbation of the H atom by neighboring H atoms and H_2 molecules. An examination of Figure 2 in Kowalski & Saumon (2006) suggests that the effect of this additional opacity on a 5800 K hydrogen-rich white dwarf corresponds to an increase of $\approx$0.25 and 0.02 mag in the u and g bands, respectively. Hence, the effect is mostly apparent in the $u-g$ color index and corresponds, as observed, to a downward vertical shift in the $u-g$ versus $g-r$ diagram.

The temperatures were derived by minimizing the χ^2 between the observed photometry and the synthetic colors. The synthetic u and g magnitudes for hydrogen-rich models were corrected by +0.25 and +0.02 mag, respectively. The errors in temperatures were determined from considering the uncertainties in the observed colors only. Therefore, the quoted errors do not take into account systematic errors in synthetic colors such as those discussed above. The observed $(u-g)$ versus $(g-r)$ colors correspond to an effective temperature of 5200 $\pm$ 100 K using the pure-hydrogen sequence, and 5300 $\pm$ 100 K using the blackbody colors. The observed $(r-i)$ versus $(g-r)$ colors correspond to an effective temperature of 5100 $\pm$ 100 K using the pure-hydrogen sequence and 5400 $\pm$ 50 K using blackbody colors.

We also fit the SDSS *ugriz* photometry to synthetic *ugriz* absolute magnitudes, and found that $T_{\rm eff} = 5300 \pm 200$ K when using the hydrogen-rich sequence (assuming $\log g = 8.0$) and $T_{\rm eff} = 5500 \pm 200$ K, assuming a blackbody. We also fit the available spectrum (3800–6190 Å) to DA spectra at $\log g = 8.0$ and blackbody spectra to obtain $T_{\rm eff} = 5100 \pm 200$ K and $T_{\rm eff} = 5580 \pm 160$ K, respectively. Figure 8 shows the spectrum and *ugriz* photometry of LP 133-374 compared to a hydrogen-rich spectrum at $T_{\rm eff} = 5100$ K and a blackbody spectrum at $T_{\rm eff} = 5500$ K.

We determined the possible range of mass values for the white dwarf assuming both hydrogen-rich atmospheres and helium-rich atmospheres (using a blackbody approximation). First, we calculated the absolute magnitude of the white dwarf based on the distance, and therefore if the system is between 42 and 56 pc, then the absolute magnitude (M_g) of the white dwarf is between 15.68 and 15.06.

Assuming the white dwarf is hydrogen-rich, then the mean of the temperatures determined above is $T_{\rm eff} = 5175 \pm 100$ K. The mass range can then be determined using the mass-radius relations of Benvenuto & Althaus (1999) with a hydrogen envelope of

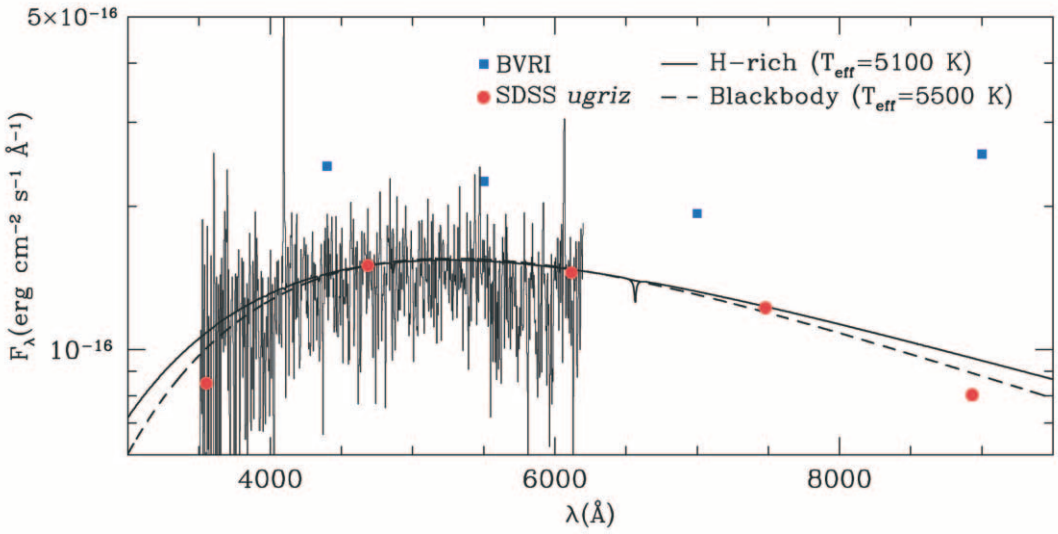

FIG. 8.—SDSS *ugriz* and *BVRI* photometry and a spectrum of LP 133-374 compared to a model DA spectrum and a blackbody spectrum. The hydrogen model shown does not include the effect of missing blue/ultraviolet opacity.

$M_H/M_\star = 10^{-4}$ and a metallicity of $Z = 0$, where for a given temperature, the absolute magnitude is a function of the radius and therefore the mass. We determined a mass of 0.49–0.70 $M_\odot$ with a cooling age ranging from 3.6×10^9 to 4.5×10^9 yr.

Assuming the white dwarf is helium-rich, and using a blackbody approximation for the energy distribution, then the mean of the temperatures determined using the different methods as discussed above is $T_{\rm eff} = 5445 \pm 120$ K. For the mass determinations in this case, we used the mass-radius relations of Benvenuto & Althaus (1999) without a hydrogen envelope and with a metallicity of $Z = 0.001$. Therefore, if LP 133-374 is a helium-rich white dwarf with $T_{\rm eff} = 5445$ K, we can estimate the mass to be between 0.55 and 0.82 $M_\odot$ and the cooling age to be between 2.7×10^9 and 4.5×10^9 yr. The progenitor of a 0.82 $M_\odot$ white dwarf is a early-type star of $\approx$4 $M_\odot$ (Weidemann 2000) with a main-sequence life time $\approx 10^8$ yr. These ages imply a minimum age of 3×10^9 yr for the LP 133-373/LP 133-374 system.

For a temperature range of 5000–5500 K, the corresponding 2MASS absolute magnitude $M_J = 13.4$–13.6, or an apparent magnitude of $m_J = 16.5$–16.7, fainter than the limiting magnitude of the 2MASS survey.

4. SUMMARY AND CONCLUSIONS

We have modeled light and velocity curves of LP 133-373 as an eclipsing binary with two similar dM-type stars with spots. Although the masses and radii of 0.340 ± 0.014 $M_\odot$ and 0.33 ± 0.02 $R_\odot$ make them appear marginally more massive and smaller than other stars of the same type tabulated by Reid & Hawley (2000), a complete radial velocity study and additional light curves are required before we can reach a conclusion on this matter. The uncertainty in the mass ratio and the paucity of velocity data create a large uncertainty in the semimajor axis and ultimately in the individual masses. The role of spots also plays a critical role in light curve modeling and the resulting fits. The 2006 May data set shows light curve variations suggesting that spot activity had significantly changed within a month. We intend to obtain high-dispersion spectra of LP 133-374 sampling a complete orbital period in the Hα region. New photometry, covering several complete orbital periods, would be helpful in constraining the geometry of the spots and the individual temperatures. The new data will provide the better mass, luminosity, and radius information that is so important for understanding low-mass stars. In addition, limb darkening of these cool stars is also important to the light curve models. A study of additional stars like these is needed to refine limb-darkening models.

The white dwarf is tentatively classified as a DC spectral type, and a possible DA type. It has a temperature of 5100–5500 K depending on the atmospheric abundance of hydrogen. Adopting the distance of its common proper motion companion LP 133-373 (42–56 pc), we constrain the radius, and hence the mass of the white dwarf. The mass of the white dwarf is estimated to be $0.49 \lesssim M/M_\odot \lesssim 0.82$. Consequently, the minimum total age of the system is 3 Gyr. The angular separation of 5″ between the white dwarf and the eclipsing binary corresponds to a projected separation of 210–280 AU. This separation excludes the possibility of past interactions.

New Hα spectroscopy will also help establish the spectral type of the white dwarf and accurately determine its physical characteristics. In turn, this will be helpful in establishing the age of the triple system from the white dwarf cooling age.

We thank KPNO for a generous allocation of observing time. We are especially grateful for the observing support of Rob Wilkos, John Robertson, and Kyle Johnston. M. R. is supported by NASA Graduate Student Research Program NGT5-50450. A. Kawka is supported by GA ČR 205/05/P186. S. V. acknowledges support from the College of Science at the Florida Institute of Technology. This work was supported in part by NSF grant AST-0206115 (T. D. Oswalt, Principal Investigator) to Florida Institute of Technology. M. W. acknowledges support from NSF grant AST-0097616. We thank S. Shaw, R. Wilson, and Casey T. Hendley for useful discussions and N. Silvestri for sharing observing time at APO. We thank the anonymous referee for several useful comments that improved the paper.

This research is also based in part on observations obtained with the Apache Point Observatory 3.5 m telescope, which is owned and operated by the Astrophysical Research Consortium (ARC). Funding for the SDSS and SDSS II has been provided by the Alfred P. Sloan Foundation, the Participating Institutions, the National Science Foundation, the U.S. Department of Energy, the National Aeronautics and Space Administration, the Japanese Monbukagakusho, the Max Planck Society, and the Higher Education Funding Council for England. The SDSS Web Site is http://www.sdss.org. This publication also makes use of data products from the Two Micron All Sky Survey, which is a joint project of the University of Massachusetts and the Infrared Processing and Analysis Center/California Institute of Technology, funded by the National Aeronautics and Space Administration and the National Science Foundation.

REFERENCES

Bayless, A. J., & Orosz, J. A. 2006, ApJ, 651, 1155
Benvenuto, O. G., & Althaus, L. G. 1999, MNRAS, 303, 30
Caillault, J.-P., & Patterson, J. 1990, AJ, 100, 825
Chabrier, G., & Baraffe, I. 2000, ARA&A, 38, 337
Cox, A. N. 2000, Allen's Astrophysical Quantities, ed. A. N. Cox (4th ed.; New York: AIP), 388
Hebb, L., Wyse, R. F. G., Gilmore, G., & Holtzman, J. 2006, AJ, 131, 555
Kawka, A., & Vennes, S. 2006, ApJ, 643, 402
Kowalski, P. M., & Saumon. D. 2006, ApJ, 651, L137
Lopez-Morales, M., & Shaw, J. S. 2006, preprint (astro-ph/0603748)
Luyten, W. J. 1979, A Catalogue of Stars with Proper Motions Exceeding 0.5″ Annually (2nd ed; Minneapolis: Univ. Minnesota)
Nidever, D. L., Marcy, G. W., Butler, R. P., Fischer, D. A., & Vogt, S. S. 2002, ApJS, 141, 503
Oswalt, T. D., Rudkin, M., Johnston, K., Kissinger, J., & Menezes, K. 2005, in ASP Conf. Ser. 334, 14th European Workshop on White Dwarfs, ed. D. Koester & S. Moehler (San Francisco: ASP), 605
Prša, A., & Zwitter, T. 2005, ApJ, 628, 426
Reid, N., & Hawley, S. L. 2000, New Light on Dark Stars: Red Dwarfs, Low Mass Stars, Brown Dwarfs (New York: Springer)
Reid, N., Hawley, S. L., & Gizis, J. E. 1995, AJ, 110, 1838
Rudkin, M. 2003, M.S. thesis, Florida Institute of Technology
Shaw, J. S., & Lopez-Morales, M. 2006, preprint (astro-ph/0603744)
Silvestri, N. M. 2002, Ph.D. thesis, Florida Institute of Technology
Silvestri, N. M., Hawley, S. L., & Oswalt, T. D. 2005, AJ, 129, 2428
Skrutskie, M. F., et al. 2006, AJ, 131, 1163
Smith, J. A. 1997, Ph.D. thesis, Florida Institute of Technology
van Hamme, W. 1993, AJ, 106, 2096
Weidemann, V. 2000, A&A, 363, 647
Wilson, R. E. 1979, ApJ, 234, 1054
———. 1990, ApJ, 356, 613
Wilson, R. E., & Devinney, E. J. 1971, ApJ, 166, 605
Young, T. B., Hidas, M. G., Webb, J. K., Ashley, M. C. B., Christiansen, J. L., Derekas, A., & Nutto, C. 2006, MNRAS, 370, 1529